

THE CRAB NEBULA: LINKING MEV SYNCHROTRON AND 50 TEV INVERSE COMPTON PHOTONS

D. Horns and F.A. Aharonian

Max-Planck-Institut für Kernphysik, D-69117 Heidelberg, Germany

ABSTRACT

Pulsar wind driven synchrotron nebulae are offering a unique view on the connection of the pulsar wind and the surrounding medium. The Crab nebula is particularly well suited for detailed studies of the different emission regions. As inferred from the observed synchrotron emission extending beyond MeV energies, the Crab is a unique and extreme accelerator. In the framework of the synchrotron/inverse Compton emission model, the same electrons with energies exceeding 10^{15} eV that are responsible for the MeV synchrotron emission produce via inverse Compton scattering 10-50 TeV radiation which has recently been observed with the HEGRA system of ground based gamma-ray telescopes. Here we discuss the close relation of the two energy bands covered by INTEGRAL and ground based gamma-ray telescopes. Despite the lack of sufficient spatial resolution in both bands to resolve the emission region, correlation of the flux measurements in the two energy bands would allow to constrain the structure of the emission region. The emission region is expected to be a very compact region (limited by the life-time of the electrons) near the termination shock of the pulsar wind. We extend previous model calculations for the nebula's emission to include an additional compact non-thermal emission region recently detected at mm wavelengths. The overall good agreement of this model with data constrains additional emission processes (ions in the wind, inverse Compton from the unshocked wind) to be of little relevance.

Key words: Crab nebula; acceleration; Crab pulsar; electrons; radiation; synchrotron; inverse Compton.

1. INTRODUCTION

Observations of the Crab pulsar and nebula have been carried out in every observationally (ground and space based) accessible wavelength band. The resulting broad band spectral energy distribution (see Fig. 1) is exceptionally complete and unique amongst all astronomical objects observed and studied. The historical lightcurve of the super nova explosion of 1054 A.D. is not conclusive with respect to the type of progenitor star that exploded and leaves many questions unanswered to the stellar evo-

lution of the progenitor star. At the present date, the observed remnant is of a plerionic type with a bright continuum nebula emission and filamentary structures emitting mainly in lines in the near infrared and optical.

The remaining compact central object is a pulsar with a period of 33 ms and a spin-down luminosity of $\propto \dot{P}^3/P = 5 \cdot 10^{38}$ erg/s. The emitted power of the continuum peaks in the hard UV/ soft X-ray at $\approx 10^{37}$ erg/s (assuming a distance of 2 kpc). Given the kinetic energy of the spinning pulsar as the only available source of energy in the system, the spin-down luminosity is efficiently converted into radiation. There is no evidence for accretion onto the compact object as an alternative mechanism to feed energy into the system.

The observed SED of the nebula is commonly interpreted as synchrotron emission from relativistic electrons. The general features of the SED are characterised by 3 breaks connecting 4 power-law type spectra. The breaks occur in the near infrared, near UV, and hard X-ray. The break frequencies are inferred indirectly because they occur in spectral bands which are difficult to observe. The high energy part of the synchrotron spectrum cuts off at a few MeV (see Fig. 1). This energy is very close to the theoretical limit for synchrotron emission derived from balancing energy gain in diffusive shock acceleration and energy losses to be $h\nu_{max} \approx m_e c^2/\alpha = 68$ MeV (independent of the magnetic field). In this sense, the Crab accelerates particle close to the extreme limit of diffusive shock acceleration. However, the interpretation of the multi MeV emission as synchrotron emission requires the presence of electrons up to PeV energies. These 0.1-1 PeV electrons inevitably radiate via inverse Compton scattering at photon energies above 50 TeV with detectable fluxes (Horns et al., 2003; Tanimori et al., 1998; Aharonian et al., 2004). Another independent indication for a common origin of MeV and TeV photons is correlated variability of the nebula emission in these two energy bands which will be discussed in Sect. 4.

The spatially resolved morphology of the nebula is of complex structure and shows a general decrease of the size of the emission region with increasing energy. However, there are indications that at mm-wavelengths, a compact, possibly non-thermal emission region is present that does not follow the general behaviour (Bandiera, Neri, & Cesaroni, 2002). The central region close to the torus-like structure is also known to

be variable in time at Radio (Bietenholz, Frail, & Hester, 2001), optical (Hester et al., 1995), and X-ray frequencies (Hester et al., 2002). The morphology of these moving structures has led to the commonly used term “wisps” (Scargle, 1969). Whereas in the radio the measured spectrum is independent of the location in the nebula, at higher frequencies, a general softening of the spectrum from the central region to the outer edge of the nebula is observed. Recent high resolution spectral imaging at X-ray energies have revealed a *hardening* of the spectrum in the torus region which could be indicative of another location of acceleration (Mori et al., 2004). This is an exciting prospect for future gamma-ray observations with better spatial resolution as will be discussed in Section 6.

The very high energy (VHE) emission observed at GeV to TeV energies is attributed to inverse Compton scatterings taking place between the electrons and various soft photon fields present. Based upon accurate measurements of this inverse Compton component, a reliable estimate of the average magnetic field can be derived resolving the degeneracy of magnetic field energy density and particle number density for the synchrotron emission. Currently, the volume averaged magnetic field is estimated to be 160 μG (Aharonian et al., 2000b).

The VHE emission above 100 GeV is only observable with ground based gamma-ray instruments. This type of instrument uses the atmospheric Cherenkov effect to record images of extended air showers with large optical telescopes. The performance and sensitivity of ground based gamma-ray instruments have improved considerably over the past decade and allow to investigate in detail the high energy end of the spectrum of the Crab nebula and pulsar. Recently, a new and detailed measurement of the VHE emission of the Crab nebula has been published by the HEGRA collaboration (Horns et al., 2003). The wide energy coverage from 500 GeV up to 50 TeV and beyond is of crucial importance to understand the origin of the emission and to observe directly the acceleration of particles to PeV energies.

In this contribution, we present new model calculations for the VHE emission based upon a phenomenological approach incorporating an additional seed photon distribution discovered at mm wavelengths (Bandiera, Neri, & Cesaroni, 2002). The model calculation will be briefly outlined in the next section. Comparison with the VHE measurements and interpretation will be given in Section 3. Finally, a discussion of expected variability at energies beyond 10 TeV and correlation with MeV synchrotron emission observable with INTEGRAL will be given followed by a discussion and an outlook.

2. MODEL CONSIDERATIONS

With the seminal papers of Rees & Gunn (1974) and Kennel & Coroniti (1984), a detailed picture of the evolution of accelerated particles and the magnetic field in the nebula based upon the magneto-hydrodynamic approximation (MHD) has evolved. In this picture, an ef-

ficient acceleration process converts spin-down power of the pulsar into a relativistic wind injected near the magnetosphere of the pulsar. Possible mechanisms could invoke electrostatic gaps which produce a dense relativistic plasma with Lorentz factors of $\gamma \approx 10^2 - 10^3$ which are then released beyond the light cylinder. In this picture, the energy carried by the radial outflow close to the magnetosphere is almost entirely dominated by its Poynting flux (the ratio of Poynting flux over kinetic energy flux $\sigma \approx 1000$).

The highly relativistic but cool flow terminates at roughly 10 arc-seconds angular distance to the pulsar when the pressure of the flow is balanced by the pressure of the nebula. Given the observation of the synchrotron emission of the nebula and the boundary conditions for the plasma parameters at the edge of the nebula, it appears that almost the entire energy of the flow far away from the magnetosphere is dominated by its kinetic energy. This dramatic and so far not well understood change of the σ parameter is commonly referred to as the “ σ problem”.

The standing reverse shock quickly isotropizes the particle distribution in the downstream frame and gives rise to a power-law type energy distribution of the particles which then adiabatically expands and dissipates energy via synchrotron emission in the downstream region. Numerous physical and observational details of this picture are still lacking a clear understanding but this model nevertheless successfully explains the spatial and energy distribution of electrons in the nebula responsible for the optical to hard X-ray emission. Observations carried out with the Chandra and XMM-Newton X-ray imaging telescopes have led to a more detailed phenomenological picture of the distribution of particles in the nebula, which has stipulated attempts to model the torus-type geometry with an asymmetric outflow (Bogovalov & Khangoulyan, 2002; Shibata et al., 2003). It appears that a purely toroidal field topology is not consistent with the observations which are indicating the presence of turbulences in the torus region.

In general, the calculation of the predicted VHE emission has been approached in two different ways in the past: As a phenomenological approach, the observed synchrotron emission has been used to extract the electron energy distribution - with some ambiguity with respect to the magnetic field present (Hillas et al., 1998; de Jager et al., 1996). In a more sophisticated approach, the MHD flow model of Kennel & Coroniti (1984) has been used to calculate the synchrotron and inverse Compton emissivities (Atoyan & Aharonian, 1996) consistently. Generally, all models give comparable results for the predicted VHE emission.

Besides differences in the approach which do not change the result of the calculation much, the calculations strongly depend on the seed photon field(s) used to calculate the inverse Compton scattering. Commonly, three different seed photon fields have been taken into account to calculate the inverse Compton emission. Here we propose a fourth one.

- Synchrotron emission: This radiation field domi-

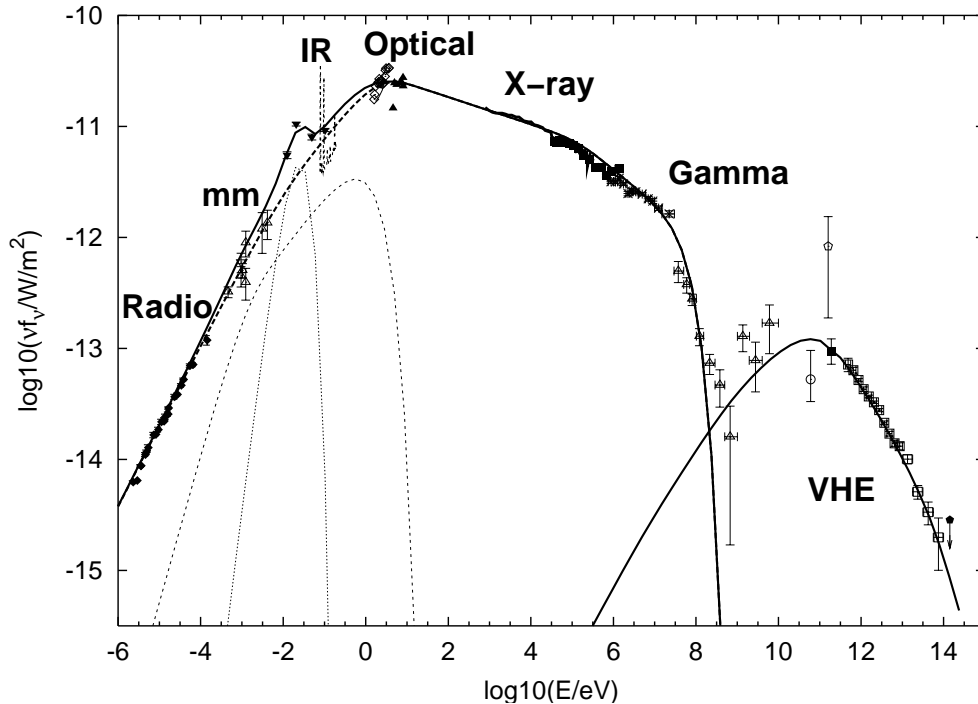


Figure 1. Given the impressive coverage of different energy bands, the Crab nebula is one of the best studied objects in multi-wavelengths. The data used for this compilation and their origin are described in the text. The solid line is the model used in this work which is the sum of the synchrotron component (thick dashed), a thermal component (short dashed), and the non-thermal synchrotron component at mm wavelengths (long dashed). The compilation is not complete but chosen such that the most recent available measurements are included. Please refer to the text for references and explanations on the selection of data.

nates in density for all energies and is the most important seed photon field present.

- Far infrared excess: Observations at far-infrared have shown the presence of thermal emission which exceeds the extrapolation of the continuum emission from the radio band. This component is best described by a single temperature of 46 K (Strom & Greidanus, 1992). Unfortunately, the spatial structure of the dust emission remains unresolved which introduces uncertainties for the model calculations. We have assumed the dust to be distributed like the filaments with a scalelength of 1.3 arcmin. Sophisticated analyses of data taken with the ISO satellite indicates that the dust emission can be resolved (Tuffs, private communication). The resulting size seems to be consistent with the value assumed here.
- Cosmic Microwave Background (CMB): Given the low energy of the CMB photons, scattering continues to take place in the Thomson regime even for electron energies exceeding 100 TeV.

Additionally, the influence of stellar light have been found to be negligible (Atoyan & Aharonian, 1996). The optical line emission of the filaments is spatially too far separated from the inner region of the nebula where the very energetic electrons are injected and cooled. However, in the case of acceleration taking place at different

places of the nebula, the line emission could be important.

The recent claim of a detection of a compact possibly nonthermal emission region at mm wavelengths in the center of the nebula (Bandiera, Neri, & Cesaroni, 2002) has stipulated us to calculate the contribution of inverse Compton scattering off of mm photons.

If the origin of the mm photons is nonthermal, it is very likely an additional synchrotron component. The electrons responsible for this component could be injected in a shock region closer to the pulsar - possible in the polar region.

Recent MHD calculations carried out by Komissarov & Lyubarsky (2003) have shown that shocks form at various distances to the pulsar. These shocked regions could efficiently inject electrons with $\gamma = 10^3 - 10^4$ which would produce the observed compact mm radiation component. At the same time, these electrons would radiate at GeV energies via inverse Compton scattering. If the region is sufficiently compact (< 10 arc-sec), the measured large GeV flux by EGRET could be well explained by this component.

It would be of great interest to investigate the spatial structure of this GeV component. Given the size of the mm region, the corresponding inverse Compton component would naturally be compact as well. However, roughly half of the observed flux is emitted by electrons

which are spread over the entire nebula and would give rise to an extended emission region. With the advent of ground and space based observatories with sufficiently good angular resolution and sensitivities at roughly 10-30 GeV, the two components could be distinguished.

Independent of the model for the injection and acceleration, it is convenient to derive the energy spectrum of the synchrotron emitting electrons from the observed continuum emission assuming an average magnetic field. The characteristic size of the synchrotron emitting region is derived from measurements and used to calculate the average photon density distribution that participate in the inverse Compton scattering. The main assumption is spherical symmetry and that the surface brightness map follows a Gaussian distribution. This approach was originally introduced by Hillas et al. (1998). The major differences with the original treatment are updates of the measurements, inclusion of an additional seed photon field, and a modification of the electron distribution to fit the break in the near IR better.

For the purpose of compiling and selecting available measurements in the literature, mostly recent measurements have been chosen. The prime goal of the compilation is to cover all possible wavelengths from radio to gamma-ray. The radio data is taken from (Baars & Hartsuijker, 1972) and references therein, mm data from (Mezger et al., 1986; Bandiera, Neri, & Cesaroni, 2002) and references therein, and the infra-red data from (Douvion, Lagage, Cesarsky, & Dwek, 2001; Strom & Greidanus, 1992).

Optical and near-UV data from the Crab nebula requires some extra considerations. The reddening along the line-of-sight towards the Crab nebula is a matter of some debate. For the sake of homogeneity, data in the optical (Veron-Cetty & Woltjer, 1993) and near-UV and UV (Hennessy et al., 1992; Wu, 1981) have been corrected applying an average extinction curve for $R = 3.1$ and $E(B - V) = 0.51$ (Cardelli, Clayton, & Mathis, 1989). This consistent treatment ensures that the data of different publications can be combined more easily.

The high energy measurements of the Crab nebula have been summarized recently in Kuiper et al. (2001) to the extent to include ROSAT HRI, BeppoSAX LECS, MECS, and PDS, COMPTEL, and EGRET measurements covering the range from soft X-rays up to gamma-ray emission. For the intermediate range of hard X-rays and soft gamma-rays, data from Earth occultation technique with the BATSE instrument have been included (Ling & Wheaton, 2003).

The available VHE emission data is a collection of non-imaging (Arqueros et al., 2002; de Naurois et al., 2002; Oser et al., 2001) and imaging ground based air shower experiments (Horns et al., 2003).

The mm-component is modeled with an angular size of 36 arc-sec as a value derived from Fig. 5 of (Bandiera, Neri, & Cesaroni, 2002). The origin of the compact component is very likely non-thermal as pointed out in Bandiera, Neri, & Cesaroni (2002). An ultra-cool (< 5 K) dust component required to match the data would

have to be unrealistically massive ($> 100 M_{\odot}$).

3. COMPARISON OF THE MODEL TO DATA

The overall broadband spectral energy distribution is described quite well by the model which is a good cross-check for the procedure (see Fig. 1). However, the good agreement is not a surprise, because the electron distribution is chosen to reproduce the data.

The prediction for the inverse Compton emission at high energies is compared with the data in Fig. 2. The different contributions of seed photons is indicated in the same picture. Obviously, the synchrotron seed photons are dominant at all energies. However, with increasing photon energies, the contribution of the CMB and notably of the mm radiation is of comparable importance as the synchrotron photon field. This is a consequence of the Klein-Nishina suppression of the inverse Compton scattering at high center of momentum energies which strongly suppresses the contribution of the higher energy synchrotron seed photons to the inverse Compton emission.

The overall agreement of the VHE prediction with the data is excellent. Over the entire range of energies above 500 GeV up to 80 TeV, the observed spectrum is well described by the model calculations. In fact, ignoring the contribution of the compact mm emission region reproduces the data still reasonably well.

The agreement of the model based upon an electron distribution inferred from the synchrotron emission is important for constraining possible other emission mechanisms present. This has a number of immediate consequences for the interpretation:

1. The presence of very energetic electrons with energies well beyond 100 TeV is required to explain the multi-TeV emission as inverse Compton radiation. The same electrons would comfortably produce the observed MeV radiation via synchrotron emission provided that the magnetic field is $O(100 \mu\text{G})$.
2. There is no indication for any additional components as expected in the presence of ions in the wind (Amato, Guetta, & Blasi, 2003).
3. There is no indication for any additional components as expected from the unshocked wind (Bogovalov & Aharonian, 2000).

Independent of the absolute flux predicted in the model and compared with the measurements, it is interesting to compare the predicted shape, namely the predicted gradual steepening of the spectrum with the observations. To do so, the differential spectra are used to calculate the slope as a function of energy.

$$\Gamma \left(\frac{\ln \nu_1 + \ln \nu_2}{2} \right) = \frac{\ln \Phi_1 - \ln \Phi_2}{\ln \nu_1 - \ln \nu_2} \quad (1)$$

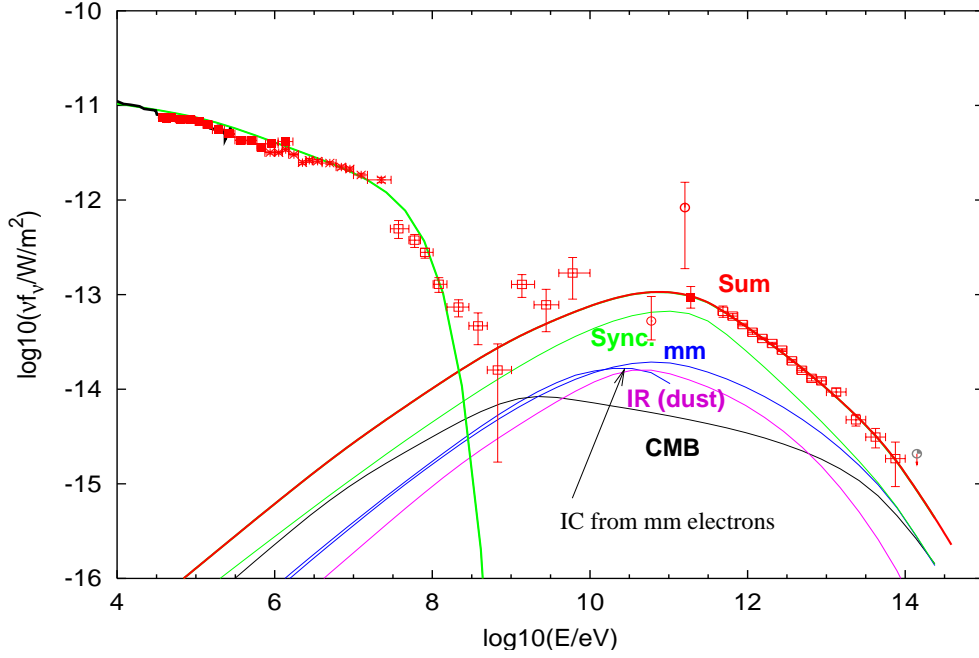


Figure 2. The VHE emission decomposed into different seed photon contributions compared with a collection of data and including the most recent VHE spectral measurement published by the HEGRA collaboration. The dominating seed photon field is the synchrotron emission. At high energies, the CMB and the mm component are of equal importance. Assuming a synchrotron origin of the mm component, the electrons produce GeV emission via inverse Compton scattering. The flux depends on the size of the mm emission region. Provided that the size is of the order of 10 arcsec the GeV flux measured by EGRET could be well matched by this model.

Based upon Eqn. 1 with error propagation assuming that the error on ν $\sigma_\nu = 0$, an estimate on the error of the photon index can be derived.

$$\sigma_\Gamma = \frac{1}{\ln \nu_1 - \ln \nu_2} \sqrt{\left(\frac{\sigma_{\Phi_1}}{\Phi_1}\right)^2 + \left(\frac{\sigma_{\Phi_2}}{\Phi_2}\right)^2} \quad (2)$$

For the data, we have chosen to calculate the logarithmic slope between data points separated by 0.625 in decadic logarithm. This is a compromise between the required leverage ($\ln \nu_1 - \ln \nu_2$) which should be sufficiently large to keep the statistical error small and still retain the sensitivity for possible changes in the slope. The resulting differential plot of slope is shown in Fig. 3 comparing the data with the model calculated here (solid line), the same model excluding the mm emission (long dashed line), and the calculation in Hillas et al. (1998).

Again, the data confirms the expected trend of the model of a gradual steepening. It is noteworthy, that the energy range covered by presently existing VHE data is sampling an energy interval which exhibits only very small changes in the photon index. With the existing data, a pure power law fit is still acceptable in terms of χ^2 -probability. However, looking at Fig. 3, it is immediately clear, that the systematic trend of the data is not following a random pattern. The slope of the model spectrum gets slightly steeper with increasing energy. Ignoring an additional contribution from a compact mm emitting region softens the spectrum slightly. Given the statistical uncertainties, both possibilities are consistent with the data. In any

case, even with the minimal assumption of the CMB field and the synchrotron photons to participate in the inverse Compton scattering, the VHE flux is well explained by electronic emission with a slightly lower magnetic field of 140 μG .

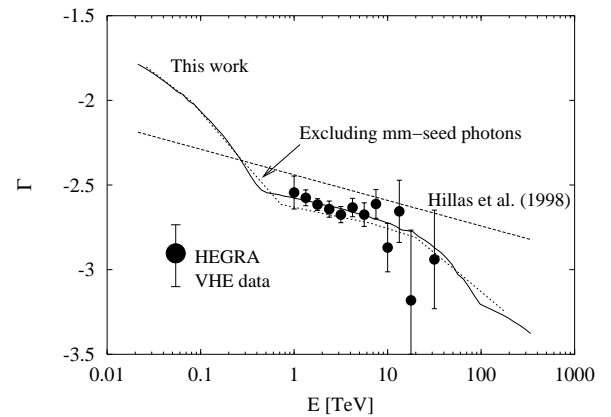


Figure 3. As a function of energy, the model presented here gives a distinct prediction for the change of the photon index. The gradual steepening of the energy spectrum in the energy range above a few hundred GeV is confirmed by the data. Note, the dashed line indicates the change of slope as it has been proposed in Hillas et al. (1998).

4. CORRELATED VARIABILITY: LINKING THE MEV AND TEV EMISSION

Together with the advent of INTEGRAL and its sensitivity up to MeV energies, it is becoming feasible to study correlated time variations in the MeV and TeV energy band. The MeV photons are emitted by electrons with typical energies exceeding 100 TeV in the average magnetic field ($\gamma = 2 \cdot 10^8 (\epsilon/400\text{keV})^{1/2} (B/160 \mu\text{G})^{-1/2}$).

Given the fast decline of the cross section for inverse Compton scattering at center of momentum energies $s^{1/2} \gg mc^2$, these electrons scatter predominantly on mm wavelength radiation producing roughly photons at energies exceeding 10 TeV. The lifetime of electrons at these energies is of the order of a few months. It seems natural to expect variations of the synchrotron flux at hundreds of keV and in fact, indications of variability have been claimed (Ling & Wheaton, 2003).

Given the short lifetime of the electrons, the emission region is expected to be spatially compact and unresolved by gamma-ray instruments in the near future. However, by finding a correlation between the two bands, it is possible to establish *directly* that the same population of electrons is responsible for the emission via synchrotron and inverse Compton scattering and constrain the size of the acceleration/emission region by measuring the typical timescale of variability.

5. SUMMARY AND CONCLUSIONS

The observations of MeV synchrotron and multi-TeV inverse Compton emission from the Crab nebula establishes the presence of energetic electrons reaching PeV energies. The mechanism responsible for accelerating electrons to PeV energies needs to be efficient and fast. The highest obtainable energy for synchrotron photons in the framework of diffusive shock acceleration in the Bohm limit is independent of the magnetic field strength and approximately 70 MeV. Given the observed steep cut-off in the spectral energy distribution of the Crab nebula at a few MeV, the accelerating mechanism present is within an order of magnitude to the theoretical limit. The recent detection of gamma-ray emission at energies exceeding 50 TeV is consistent with the expectation for inverse Compton emission. At energies beyond 50 TeV, soft seed photons at mm wavelengths are of similar importance as the synchrotron seed photons. The presence of ions in the wind is not evident from the comparison of the data with the model. In some models, ions in the wind are invoked to explain the surprisingly high efficiency of acceleration of electrons (positrons) in the shock (Hoshino et al., 1992). These ions should carry a substantial amount of the total energy flux of the wind. In principle, the unshocked wind of electrons would give rise to bulk Comptonization of the intense photon field emitted from the pulsar's surface (Bogovalov & Aharonian, 2000). Again, the good agreement of data and the model presented here, leave no "room" for these additional components unless the

wind's Lorentz factor exceeds $\approx 10^7$. Finally, if the mm emission is confirmed and its spatial structure better known, it is interesting to note that if this component is emitted by electrons, these electrons could naturally explain via inverse Compton scattering the excess of the GeV flux compared with the current model calculations.

6. OUTLOOK AND PERSPECTIVE

The long history of observations of the Crab nebula with subsequent surprises continues. With the advent of better spatial resolution at mm wavelengths an important conclusion for VHE emission can be drawn. More and better observations at mm wavelengths are needed to study the structure of the shock waves in the wind termination zone. In fact, given the spatial spectral resolution at various wavelengths, dramatic improvement of the understanding of the particles' injection, transport, and cooling in the nebula is to be expected. Given the recent X-ray observations which show the hardest spectrum in the torus of the nebula far away from the inner ring which has been commonly associated with the site of acceleration, very exciting times for gamma-ray observations are expected. In fact, if acceleration takes place at the torus, the size of the VHE emitting region could be larger than originally calculated based upon the assumption that the inner ring is the exclusive site of acceleration. With the advent of the new ground and space based gamma-ray detectors, this structure might be resolvable.

Finally, the observation of temporal correlation between the MeV and 50 TeV emission of the nebula will give us important insight into the extreme accelerator which powers the Crab nebula. We expect that especially ground based Cherenkov telescopes operating in the southern hemisphere (CANGAROO, H.E.S.S.) will collect efficiently with large collection areas of more than 1 km² these very energetic photons. It is expected, that the Crab will be often observed as a calibration target for INTEGRAL and ground based detectors. This database of observations over many years will allow to study variability and correlations which are expected given the lifetime of the electrons responsible for the emission.

ACKNOWLEDGMENTS

The authors would like to thank the organizers of the meeting for their great work.

REFERENCES

- Aharonian, F. A., Akhperjanian, A.G., Barrio, J.A. et al. 2000, ApJ, 539, 317
- Aharonian, F. A. , Akhperjanian, A.G., Beilicke, M. et al. 2004, ApJ in press
- Amato, E., Guetta, D., & Blasi, P. 2003, A&A, 402, 827
- Arqueros, F. et al. 2002, Astroparticle Physics, 17, 293

- Atoyan, A. M. & Aharonian, F. A. 1996, MNRAS, 278, 525
- Baars, J. W. M. & Hartsuijker, A. P. 1972, A&A, 17, 172
- Bandiera, R., Neri, R., & Cesaroni, R. 2002, A&A, 386, 1044
- Bietenholz, M. F., Frail, D. A., & Hester, J. J. 2001, ApJ, 560, 254
- Bogovalov, S. V. & Aharonian, F. A. 2000, MNRAS, 313, 504
- Bogovalov, S. V. & Khangoulyan, D. V. 2002, Astronomy Letters, 28, 373
- Cardelli, J. A., Clayton, G. C., & Mathis, J. S. 1989, ApJ, 345, 245
- de Naurois, M. et al. 2002, ApJ, 566, 343
- de Jager, O. C., Harding, A. K., Michelson, P. F., Nel, H. I., Nolan, P. L., Sreekumar, P., & Thompson, D. J. 1996, ApJ, 457, 253
- Douvion, T., Lagage, P. O., Cesarsky, C. J., & Dwek, E. 2001, A&A, 373, 28
- Hennessy, G. S. et al. 1992, ApJ Letters, 395, L13
- Hester, J. J., et al. 1995, ApJ, 448, 240
- Hester, J. J., et al. 2002, ApJ, 577, L49
- Hillas, A. M. et al. 1998, ApJ, 503, 744
- Horns, D. et al. in: Kifune, T.(ed) Procs. 28th International Cosmic Ray Conference, 2003 Tsukuba, Vol. 5, p 2373
- Hoshino, M., Arons, J., Gallant, Y., and B. Langdon 1992 ApJ 390, 454
- Kennel, C. F. & Coroniti, F. V. 1984, ApJ, 283, 694
- Komissarov, S. S., and Lyubarsky, Y. E. 2003 MNRAS 344, L93
- Kuiper, L., Hermsen, W., Cusumano, G., Diehl, R., Schönfelder, V., Strong, A., Bennett, K., & McConnell, M. L. 2001, A&A, 378, 918
- Ling, J. C. & Wheaton, W. A. 2003, ApJ, 598, 334
- Mezger, P. G., Tuffs, R. J., Chini, R., Kreysa, E., & Gemuend, H.-P. 1986, A&A, 167, 145
- Mori, K., Burrows, D. N., Hester, J. J., Pavlov, G. G., Shibata, S., & Tsunemi, H. 2004, ArXiv Astrophysics e-prints, astro-ph/0403287
- Oser, S. et al. 2001, ApJ, 547, 949
- Rees, M. J. & Gunn, J. E. 1974, MNRAS, 167, 1
- Scargle, J. D. 1969, ApJ, 156, 401
- Shibata, S., Tomatsuri, H., Shimanuki, M., Saito, K., & Mori, K. 2003, MNRAS, 346, 841
- Strom, R. G. & Greidanus, H. 1992, Nature, 358, 654
- Tanimori, T., et al. 1998, ApJ, 492, L33
- Veron-Cetty, M. P. & Woltjer, L. 1993, A&A, 270, 370
- Wu, C.-C. 1981, ApJ, 245, 581